Available online at www.sciencedirect.com
ScienceDirect
Nuclear Physics B Proceedings Supplement 00 (2012) 1–6
Nuclear Physics B Proceedings Supplement

Rare decays at LHCb

D. Hutchcroft, on behalf of the LHCb collaboration

Department of Physics, University of Liverpool, Oxford Street, Liverpool, L69 7ZE, UK

Abstract

Using 1.0 fb^{-1} of LHCb data, searches for the rare decays $B^0_{(s)} \to \mu^+\mu^-$, $B^0_{(s)} \to \mu^+\mu^-\mu^+\mu^-$ and $\tau^- \to \mu^+\mu^-\mu^-$ are presented. A search for $D^0 \to \mu^+\mu^-$ using 0.9 fb^{-1} of LHCb data is also discussed. In the absence of an excess of events, upper limits are set on each decay mode. Both the angular analysis of $B^0 \to K^{*0}\mu^+\mu^-$ and a measurement of the isospin asymmetries in $B \to K^{(*)}\mu^+\mu^-$ are made with 1.0 fb^{-1} of LHCb data. The measured angular and isospin observables are presented as a function of the invariant mass of the muon pairs.

Keywords: LHC-B, rare decay
PACS: 13.20.Fc, 13.20.He, 13.35.Dx

1. Introduction

The LHCb detector [1] is a detector measuring pp collisions at the Large Hadron Collider [2] in a unique pseudo-rapidity range of $2 < \eta < 5$. The detector has a high precision vertex detector, four tracking stations, two RICH detectors, a dipole magnetic field, a four layer calorimeter and a five layer muon system.

Rare decays of particles can be windows into higher mass states, as variations from the Standard Model (SM) expectations for decay rates and angular distributions may indicate heavy particles in loops. In the absence of an excess these measurements strongly constrain beyond the standard model theories. LHCb collected 1.0 fb^{-1} in 2011. The hardware stage of the LHCb trigger [1] runs on every bunch crossing and the muon triggers accept all events with one muon with $p_T > 1.5$ GeV/c or two muons which satisfy $\sqrt{p_{T1} \cdot p_{T2}} > 1.3$ GeV/c.

Each of the searches is done in a blinded fashion with a control channel used to optimise the selection on data, with the expected number of events (if any) set from the SM prediction.

2. $B^0_{(s)} \to \mu^+\mu^-$

The decays of the B^0_s and B^0 to a pair of muons[1] have a very small branching fraction in the SM, with the prediction $\mathcal{B}(B^0_s \to \mu^+\mu^-) = (3.2 \pm 0.2) \cdot 10^{-9}$ and $\mathcal{B}(B^0 \to \mu^+\mu^-) = (0.10 \pm 0.01) \cdot 10^{-9}$ [3, 4]. A search for these decays was performed with 1.0 fb^{-1} of data collected by LHCb [5]. The selection was based on a 9 variable boosted decision tree (BDT) designed to find a pair of opposite charged muons from a secondary vertex, well separated to the primary vertex, and having kinematics consistent with the expected decay. The BDT was calibrated on $B^0_{(s)} \to h^+h'^-$ (where h is a π or K), without requiring the muon track identification, to understand the peaking signal and background components, and $b\bar{b} \to \mu^+\mu^- X$ for the non-resonant backgrounds.

The background for the selection was evaluated using sidebands in $m(\mu^+\mu^-)$ extrapolated into the signal region for each bin in the BDT output. The results for BDT > 0.5 are shown in Fig 1.

The branching ratio is normalised to the rates of $B^+ \to J/\psi K^+$, $B^0_s \to J/\psi\phi$ and $B^0 \to K^+\pi^-$ decays.

[1] Charge conjugation is assumed throughout.

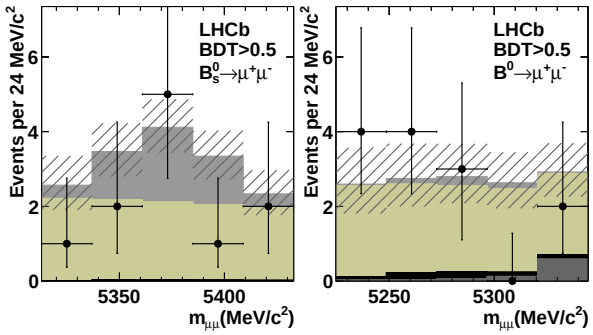

Figure 1: Distribution of data (points) for $B_s^0 \to \mu^+\mu^-$ (left) and $B_s^0 \to \mu^+\mu^-$ (right) with the estimated signal (dark grey band) and backgrounds overlaid. The darker gray bands on the $B^0 \to \mu^+\mu^-$ plot are cross-feed and the hatching indicates the uncertainty in the SM expectation.

Mode	Limit	at 95% C.L.
$B_s^0 \to \mu^+\mu^-$	Exp. bkg + SM	$7.2 \cdot 10^{-9}$
	Exp. bkg	$3.4 \cdot 10^{-9}$
	Observed	$4.5 \cdot 10^{-9}$
$B^0 \to \mu^+\mu^-$	Exp. bkg	$1.1 \cdot 10^{-9}$
	Observed	$1.0 \cdot 10^{-9}$

Table 1: Expected and observed limits on the $B_{(s)}^0 \to \mu^+\mu^-$ decays.

The upper limits on the branching ratios are given in Table 1.

A combination of this results with the other LHC experiments CMS [6] and ATLAS [7] gives the limits at 95% C.L. of $\mathcal{B}(B_s^0 \to \mu^+\mu^-) < 4.2 \cdot 10^{-9}$ and $\mathcal{B}(B^0 \to \mu^+\mu^-) < 0.81 \cdot 10^{-9}$ [8].

3. $B_{(s)}^0 \to \mu^+\mu^-\mu^+\mu^-$

The decays of B_s^0 to four muons is expected to proceed through the resonant mode $B_s^0 \to J/\psi\,\phi$ with $\mathcal{B} = (2.3 \pm 0.9) \cdot 10^{-8}$ [9]. The non-resonant decays of B^0 and B_s^0 to four muons are strongly suppressed in the standard model with the branching fraction not expected to exceed 10^{-10}. LHCb has conducted a search for these decays [10]. The resonant decays $B_s^0 \to J/\psi(\mu^+\mu^-)\phi(\mu^+\mu^-)$ and $B^0 \to K^*J/\psi$ were used to tune the selection. In total 6 events were reconstructed which were compatible with $B_s^0 \to J/\psi\,\phi$. The invariant mass distribution of the non-resonant candidates is shown in Fig 2, with no events in the B_s^0 and one in the B^0 mass window. Limits can be set at the 95% C.L., which are $\mathcal{B}(B_s^0 \to \mu^+\mu^-\mu^+\mu^-) < 1.3 \cdot 10^{-8}$ and $\mathcal{B}(B^0 \to \mu^+\mu^-\mu^+\mu^-) < 5.4 \cdot 10^{-9}$.

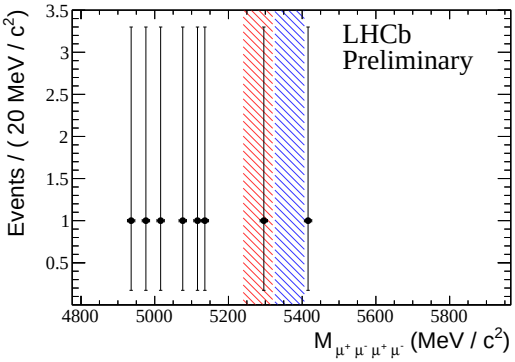

Figure 2: Distribution of data (points) for the masses of non-resonant $\mu^+\mu^-\mu^+\mu^-$ final states. The blue (right) is the B_s^0 and the red (left) is the B^0 mass window.

4. $D^0 \to \mu^+\mu^-$

In the standard model the GIM mechanism suppresses the decay $D^0 \to \mu^+\mu^-$ and it is expected to proceed almost exclusively via a long range interaction of a two photon intermediate state. The expected rate is $\mathcal{B}(D^0 \to \mu^+\mu^-) \approx 2.7 \cdot 10^{-5} \times \mathcal{B}(D^0 \to \gamma\gamma)$. The experimental limit on $\mathcal{B}(D^0 \to \gamma\gamma)$ is $2.2 \cdot 10^{-6}$ at the 90% C.L. [11], which corresponds to a SM upper limit of $\mathcal{B}(D^0 \to \mu^+\mu^-) < 6 \cdot 10^{-11}$.

The decay was searched for in the LHCb data [12], the reconstruction uses the decay chain $D^{*+} \to D^0(\mu^+\mu^-)\pi^+$ using the mass difference between the $D^{*\pm}$ and the D^0 as a strong background discriminant. $D^{*+} \to D^0(\pi^+\pi^-)\pi^+$, $D^{*+} \to D^0(K^+\pi^-)\pi^+$ and $J/\psi \to \mu^+\mu^-$ are all used as normalisation and control channels. The primary peaking background is $D^0 \to h^+h'^-$ with the hadrons decaying in flight to muons. A multivariate analysis to was applied to reduce the continuum background, predominately from semi-leptonic decays of $b-$ and $c-$hadrons, and a very tight particle identification is used to reduce the peaking background. The signal branching fraction is normalised to $\mathcal{B}(D^0 \to \pi^+\pi^-)$.

The distributions of $\Delta m = m(\mu\mu\pi) - m(\mu\mu)$ and $m(\mu\mu)$ for the events passing the selection are shown in Fig. 3. There is no excess above the expected background, so an upper limit on the branching fraction is set at a 95% C.L. of $\mathcal{B}(D^0 \to \mu^+\mu^-) < 1.3 \cdot 10^{-8}$.

5. $\tau^- \to \mu^+\mu^-\mu^-$

The lepton number violating decay of $\tau^- \to \mu^+\mu^-\mu^-$ has been searched for in the LHCb data [13]. Since the

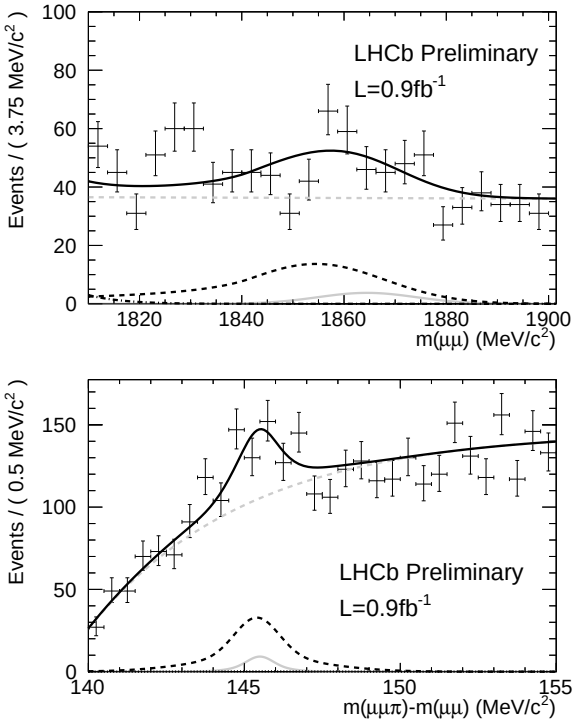

Figure 3: Distributions of $m(\mu\mu)$ (upper) and Δm (lower). The data are shown as points with error bars. The solid curve is the fit, with the following components: the combinatoric background (grey dashed line), $D^{*+} \to D^0(\pi^+\pi^-)\pi^+$ (dashed dark grey line) and the signal distribution $D^{*-} \to D^0(\mu^+\mu^-)\pi^-$ (pale grey solid line). The signal yield is consistent with zero.

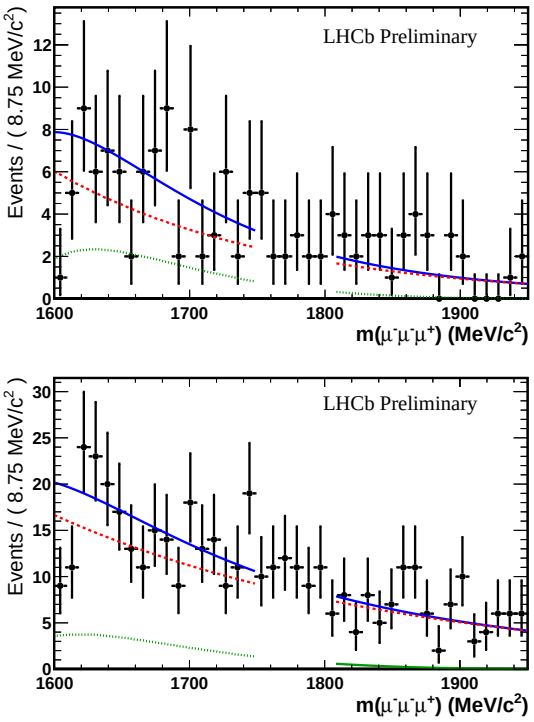

Figure 4: The observed data (points) for the reconstructed τ^- mass in the four highest signal fraction MVA bins (upper) and four next-highest bins (lower). The solid line is the combined PDF of the background, with the combinatoric (dashed) and $D_s^- \to \eta(\mu^+\mu^-\gamma)\mu^-\bar{\nu}_\mu$ (fine dotted) components shown. The signal region was excluded when fitting for the background PDF shapes.

discovery of neutrino oscillation, lepton number violating decays are known to be possible in the SM, although the expectation is that $\mathcal{B}(\tau^- \to \mu^+\mu^-\mu^-) < 10^{-40}$. Any measureable branching ratio would indicate new physics (NP) processes. The control channel for this decay is $D_s^+ \to \phi(\mu^+\mu^-)\pi^+$ which, like the signal, is selected by a multi-variate analysis (MVA) tuned for three track secondary vertices and a second MVA based around the muon identification criteria. The final fit is performed over the reconstructed mass of the τ^-.

The final branching ratio is calculated using the formula

$$\mathcal{B}(\tau^- \to \mu^+\mu^-\mu^-) = \mathcal{B}(D_s^- \to \phi(\mu^+\mu^-)\pi^-) \times \frac{f^\tau_{D_s}}{\mathcal{B}(D_s^- \to \tau^-\bar{\nu}_\tau)} \times \frac{\epsilon_{\rm cal}}{\epsilon_{\rm sig}} \times \frac{N_{\rm sig}}{N_{\rm cal}}, \quad (1)$$

where $f^\tau_{D_s}$ is the fraction of τ^- leptons originating from D_s^- decays, estimated from the cc and bb cross-sections measured at LHCb [14, 15] and the inclusive $\mathcal{B}(c \to \tau^- X)$ and $\mathcal{B}(b \to \tau^- X)$ from LEP measurements [9]. The rate of τ^- leptons from D_s^- decays was taken from [16], and the $\mathcal{B}(D_s^- \to \phi(\mu^+\mu^-)\pi^-)$ is calculated from $\mathcal{B}(D_s^- \to \phi(K^+K^-)\pi^-)$ [17] and the correction for the ratio $\mathcal{B}(\phi \to \mu^+\mu^-)/\mathcal{B}(\phi \to K^+K^-)$. $\epsilon_{\rm cal}/\epsilon_{\rm sig}$ is the efficiency ratio of the control channel and the signal, $N_{\rm sig}/N_{\rm cal}$ is the ratio of reconstructed signal and control channel events.

The data is split into five equal occupancy bins in both of the MVA outputs, then fit for the expected signal fraction and backgrounds in each of the 25 bins. Fig. 4 shows the backgrounds and signal regions for the most signal enhanced part of the data. In the absence of an excess over the background a limit is set at the 95(90)% C.L. of $\mathcal{B}(\tau^- \to \mu^+\mu^-\mu^-) < 7.8(6.3) \cdot 10^{-8}$, which is a long way above the expected SM rate. This does not improve the limit of $2.1 \cdot 10^{-8}$ at 90% C.L. set by BaBar [18].

6. Isospin of $B \to K^{(*)}\mu^+\mu^-$

The decay $B \to K^{(*)}\mu^+\mu^-$ provides a sensitive test of the physics of flavour changing neutral currents that occur in electro-weak loops. By measuring the isospin asymmetry in the decay $B \to K^{(*)}\mu^+\mu^-$ and the angular dependence of the decay $B^0 \to K^{*0}\mu^+\mu^-$, as a function of the invariant mass of the muon system (q^2), constraints on NP processes can be set based on their interaction structure, in a relatively model independent way.

In this decay the isospin asymmetry is defined as

$$A_I = \frac{\mathcal{B}(B^0 \to K^{(*)0}\mu^+\mu^-) - \frac{\tau_0}{\tau_+}\mathcal{B}(B^+ \to K^{(*)+}\mu^+\mu^-)}{\mathcal{B}(B^0 \to K^{(*)0}\mu^+\mu^-) + \frac{\tau_0}{\tau_+}\mathcal{B}(B^+ \to K^{(*)+}\mu^+\mu^-)} \quad (2)$$

where $\mathcal{B}(B \to f)$ are the branching fractions of the decays while τ_0/τ_+ is the ratio of the lifetimes of the B^0 and B^+. The SM prediction for A_I is around 1% for the q^2 region below the J/ψ resonance, rising to $O(10\%)$ as q^2 approaches zero [19].

The isospin asymmetries are determined [20] by measuring the differential branching ratios of $B^0 \to K^0_S\mu^+\mu^-$, $B^+ \to K^+\mu^+\mu^-$, $B^0 \to K^{*0}(K^+\pi^-)\mu^+\mu^-$ and $B^+ \to K^{*+}(K^0_S\pi^+)\mu^+\mu^-$. The decays with K^0_L and π^0 in the final states are not reconstructed and corrections are applied for the missing modes. Each selection is normalised to the corresponding $B \to J/\psi K^{(*)}$ channel, with the correction for the ratio of the efficiencies, as a function of q^2, taken from the Monte Carlo (MC). The selections are optimised on MC events, with corrections applied where differences between data and MC arise.

The differential $\mathcal{B}$ for $B^0 \to K^0\mu^+\mu^-$ and $B^+ \to K^{*+}\mu^+\mu^-$ are shown in Fig. 5, along with the theoretical estimates of the branching ratios. The isospin asymmetries for $B \to K\mu^+\mu^-$ and $B \to K^*\mu^+\mu^-$ are plotted in Fig. 6. For $B \to K^*\mu^+\mu^-$ the result is consistent with the very small SM expectation, in the case of $B \to K\mu^+\mu^-$ the measurement is measured to be mostly negative with a significance of $4.4\,\sigma$ from zero when integrated across q^2, consistent with previous experiments.

7. Angular analysis of $B^0 \to K^{*0}\mu^+\mu^-$

The full differential analysis of the decay $B^0 \to K^{*0}\mu^+\mu^-$ involves the following angles and variables [24]: θ_K is the helicity angle of the K^*, θ_ℓ is the helicity angle of the muon pair, $\hat{\phi}$ is the folded angle between the dimuon and K^* decay planes[2], F_L is the transverse asymmetry, A_{FB} is the forward/backward asymmetry in the dimuon system, S_3 is the transverse asymmetry and S_9 is the CP average of $A_{\rm Im}$.

[2] $\hat{\phi}$ is defined so that $\hat{\phi} = \phi + \pi$ if $\phi < 0$ and $\hat{\phi} = \phi$ otherwise

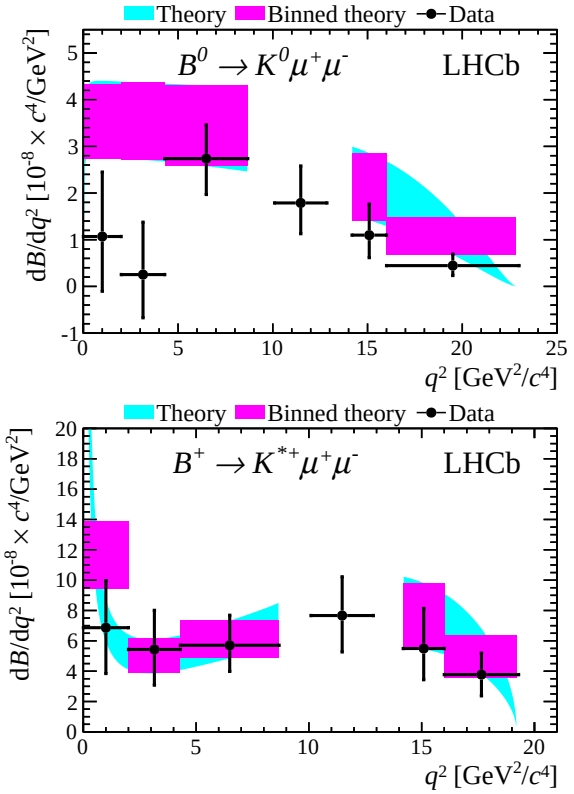

Figure 5: Differential branching ratios for $B^0 \to K^0\mu^+\mu^-$ (upper) and $B^+ \to K^{*+}\mu^+\mu^-$ (lower). The theoretical predictions are taken from Refs. [21, 22].

These are fitted using the following formula

$$\begin{aligned}
&\frac{1}{\Gamma}\frac{\mathrm{d}^4\Gamma}{\mathrm{d}\cos\theta_\ell\,\mathrm{d}\cos\theta_K\,\mathrm{d}\hat{\phi}\,\mathrm{d}q^2} = \\
&\frac{9}{16\pi}\Big[F_L\cos^2\theta_K + \frac{3}{4}(1-F_L)(1-\cos^2\theta_K) - \\
&\quad F_L\cos^2\theta_K(2\cos^2\theta_\ell - 1) + \\
&\quad \frac{1}{4}(1-F_L)(1-\cos^2\theta_K)(2\cos^2\theta_\ell - 1) + \\
&\quad S_3(1-\cos^2\theta_K)(1-\cos^2\theta_\ell)\cos 2\hat{\phi} + \\
&\quad \frac{4}{3}A_{FB}(1-\cos^2\theta_K)\cos\theta_\ell + \\
&\quad S_9(1-\cos^2\theta_K)(1-\cos^2\theta_\ell)\sin 2\hat{\phi}\Big].
\end{aligned} \quad (3)$$

The zero-point crossing of the forward/background asymmetry can be sensitive to new physics, Fig. 7 shows the measurement of the q^2_0 point. The unbinned estima-

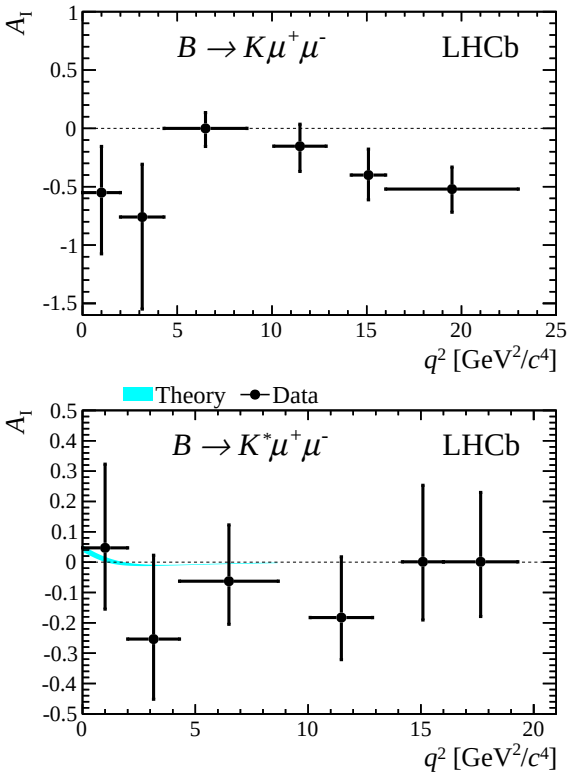

Figure 6: Isospin asymmetries for $B \to K\mu^+\mu^-$ (upper) and $B \to K^*\mu^+\mu^-$ (lower). The theoretical predictions for $B \to K^*\mu^+\mu^-$ are taken from Ref. [23].

tion of this quantity is fitted from the data and measured to be $q_0^2 = (4.9^{+1.1}_{-1.3})\,\mathrm{GeV}^2/c^4$, this is consistent with the predictions from the SM [21]. Plots of the four fitted parameters as a function of q^2 are shown in Fig. 8.

8. Conclusion

Searches for rare decays in LHCb have been performed for the decays of B_s^0, B^0 and D^0 to a pair of muons, the lepton flavour changing decay of $\tau^\pm$ to three muons and B_s^0 or B^0 to four muons. In all cases the data were compatible with the SM backgrounds and upper limits are placed on the branching ratios of these decays. Each measurement constrains NP models that postulate heavier particles which would increase the observed $\mathcal{B}$.

The isospin asymmetry of the decays of $B \to K\mu^+\mu^-$ have been measured, for the decays to $K^*\mu\mu$ the data confirm the near zero expected SM asymmetry, for the $K\mu\mu$ decays the data shows an overall negative asymmetry with $4.4\,\sigma$ significance from zero. The angular analysis of $B^0 \to K^{*0}\mu^+\mu^-$ looked at four parameters in the

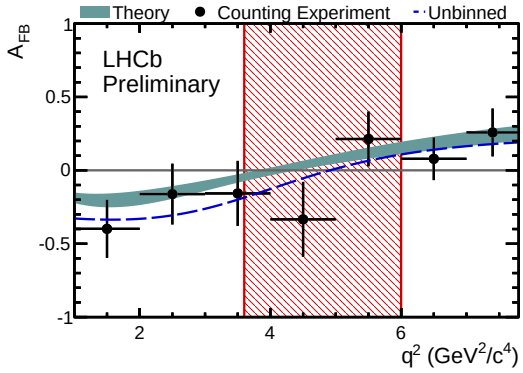

Figure 7: The A_{FB} as a function of q^2, that comes from the unbinned counting experiment (blue dashed line) overlaid with the theory prediction from Ref. [21]. The uncertainty on the data-points is statistical only. The red-hatched region is the 68% confidence interval on the zero-crossing point observed in the data.

decay as a function of q^2 and these are compatible with the SM predictions. The first measurement of the crossing point of A_{FB} has been made, $q_0^2 = (4.9^{+1.1}_{-1.3})\,\mathrm{GeV}^2/c^4$, which is compatible with the SM and not offset as several NP models predicted.

References

[1] J. Alves, A. Augusto, et al., The LHCb Detector at the LHC, JINST 3 (2008) S08005. doi:10.1088/1748-0221/3/08/S08005.
[2] Evans, L., (ed.) and Bryant, P., (ed.), LHC Machine, JINST 3 (2008) S08001. doi:10.1088/1748-0221/3/08/S08001.
[3] A. J. Buras, M. V. Carlucci, S. Gori, G. Isidori, Higgs-mediated FCNCs: Natural Flavour Conservation vs. Minimal Flavour Violation, JHEP 1010 (2010) 009. arXiv:1005.5310, doi:10.1007/JHEP10(2010)009.
[4] A. J. Buras, Minimal flavour violation and beyond: Towards a flavour code for short distance dynamics, Acta Phys.Polon. B41 (2010) 2487–2561. arXiv:1012.1447.
[5] R. Aaij, et al., Strong constraints on the rare decays $B_s^0 \to \mu^+\mu^-$ and $B^0 \to \mu^+\mu^-$, Phys.Rev.Lett. 108 (2012) 231801. arXiv:1203.4493.
[6] S. Chatrchyan, et al., The CMS experiment at the CERN LHC, JINST 3 (2008) S08004. doi:10.1088/1748-0221/3/08/S08004.
[7] G. Aad, et al., The ATLAS Experiment at the CERN Large Hadron Collider, JINST 3 (2008) S08003. doi:10.1088/1748-0221/3/08/S08003.
[8] The LHCb, CMS and ATLAS Collaborations, Search for the rare decays $B_{(s)}^0 \to \mu^+\mu^-$ at the LHC with the ATLAS, CMS and LHCb experiments, CERN-LHCb-CONF-2012-017.
[9] J. Beringer et al. (Particle Data Group), The Review of Particle Physics, Phys. Rev. D86 (2012) 010001.
[10] The LHCb Collaboration, Search for the rare decays $B_s^0 \to \mu^+\mu^-\mu^+\mu^-$ and $B^0 \to \mu^+\mu^-\mu^+\mu^-$, LHCb-CONF-2012-010.
[11] J. Lees, et al., Search for the Decay $D^0 \to \gamma\gamma$ and Measurement of the Branching Fraction for $D^0 \to \pi^0\pi^0$, Phys.Rev. D85 (2012) 091107. arXiv:1110.6480, doi:10.1103/PhysRevD.85.091107.

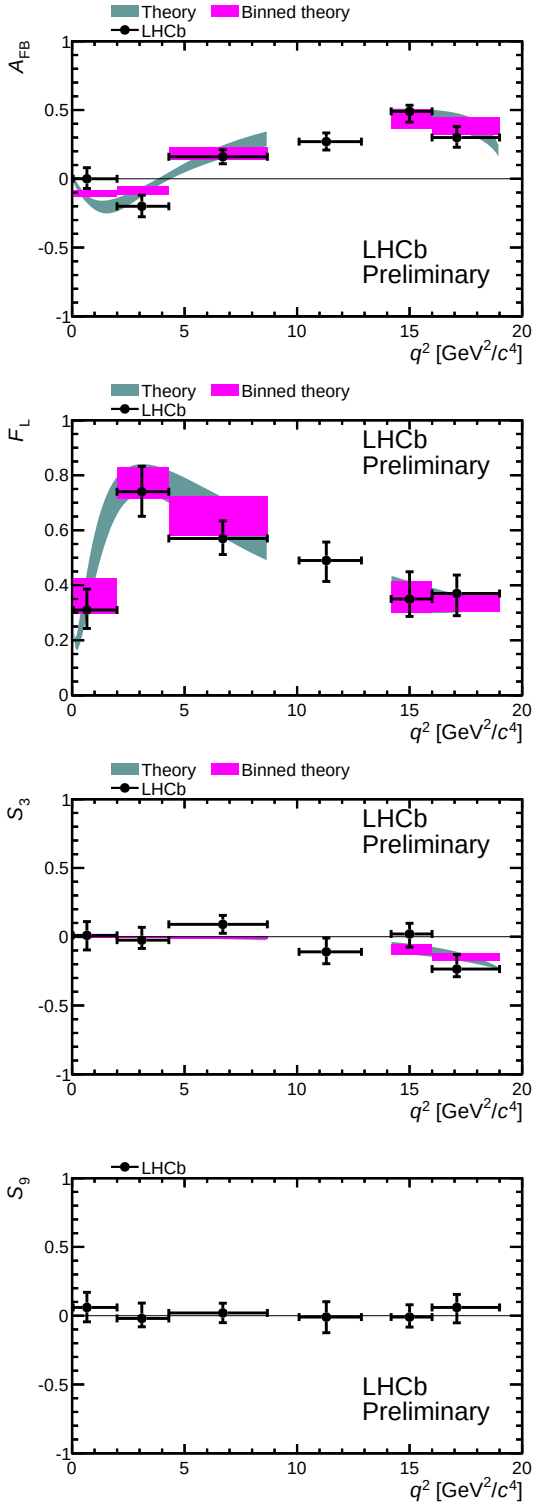

Figure 8: The distributions of A_{FB}, F_L, S_3 and S_9 for the decay $B^0 \to K^{*0}\mu^+\mu^-$. Where available the theory estimates are overlaid from Ref. [21].

[12] The LHCb Collaboration, Search for the $D^0 \to \mu^+\mu^-$ decay with 0.9 fb^{-1} at LHCb, LHCb-CONF-2012-010.

[13] The LHCb Collaboration, Search for the lepton flavour violating decay $\tau^- \to \mu^+\mu^-\mu^-$, LHCb-CONF-2012-015.

[14] R. Aaij, et al., Observation of J/ψ pair production in pp collisions at $\sqrt{s}$ = 7 TeV, Phys.Lett. B707 (2012) 52–59. arXiv:1109.0963, doi:10.1016/j.physletb.2011.12.015.

[15] The LHCb Collaboration, Prompt charm production in pp collisions, LHCb-CONF-2010-013.

[16] J. L. Rosner, S. Stone, Leptonic decays of charged pseudoscalar mesons - 2012 arXiv:1201.2401.

[17] P. del Amo Sanchez, et al., Dalitz plot analysis of $D_s^+ \to K^+K^-\pi^+$, Phys.Rev. D83 (2011) 052001. arXiv:1011.4190, doi:10.1103/PhysRevD.83.052001.

[18] K. Hayasaka, K. Inami, Y. Miyazaki, K. Arinstein, V. Aulchenko, et al., Search for Lepton Flavor Violating Tau Decays into Three Leptons with 719 Million Produced $\tau^+\tau^-$ Pairs, Phys.Lett. B687 (2010) 139–143. arXiv:1001.3221, doi:10.1016/j.physletb.2010.03.037.

[19] T. Feldmann, J. Matias, Forward backward and isospin asymmetry for $B \to K^*l^+l^-$ decay in the standard model and in supersymmetry, JHEP 0301 (2003) 074. arXiv:hep-ph/0212158.

[20] R. Aaij, et al., Measurement of the isospin asymmetry in $B \to K^{(*)}\mu^+\mu^-$ decays, JHEP 1207 (2012) 133. arXiv:1205.3422, doi:10.1007/JHEP07(2012)133.

[21] C. Bobeth, G. Hiller, D. van Dyk, More Benefits of Semileptonic Rare B Decays at Low Recoil: CP Violation, JHEP 1107 (2011) 067. arXiv:1105.0376, doi:10.1007/JHEP07(2011)067.

[22] C. Bobeth, G. Hiller, D. van Dyk, C. Wacker, The Decay $B \to Kl^+l^-$ at Low Hadronic Recoil and Model-Independent $\Delta B = 1$ Constraints, JHEP 1201 (2012) 107. arXiv:1111.2558, doi:10.1007/JHEP01(2012)107.

[23] C. Bobeth, G. Hiller, D. van Dyk, Private communication.

[24] The LHCb Collaboration, Differential branching fraction and angular analysis of the $B^0 \to K^{*0}\mu^+\mu^-$ decay, LHCb-CONF-2010-013.